Desalination and Water Treatment
www.deswater.com

doi: 10.5004/dwt.2017.21603

94 (2017) 244–253
October

Hydroxy-aluminium and cetyltrimethyl ammonium bromide modified bentonite as adsorbent and its adsorption for Orange II

Dandan Xu, Wenyun Li, Kewang Wang, Yunshan Bai, Qingwen Lin, Mengfan Gao, Hongzhu Ma*

Key Laboratory of Applied Surface and Colloid Chemistry, Ministry of Education; School of Chemistry and Chemical Engineering, Shaanxi Normal University, Xi'An, Shaanxi, 710119, China, Tel. +86 29 81530726, Fax +86 29 81530727, email: hzmachem@snnu.edu.cn

Received 1 June 2017; Accepted 31 October 2017

ABSTRACT

An inorganic-organic hybrid bentonite-based adsorbent, hydroxy-aluminium and cetyltrimethyl ammonium bromide combined modified bentonite composite (CTAB-Al-Bent), was synthesized and characterized. The adsorption properties and possible mechanism of CTAB-Al-Bent toward anionic dye, Orange II, were investigated. The influences of various experimental parameters, such as contact time, temperature, initial concentration of dye, initial pH and adsorbent dosages on Orange II removal were studied. At the optimal condition: 30 min, 303 K, 50 mg L^{-1} Orange II at pH 3.08, 0.02 g/50 mL CTAB-Al-Bent, 88.84% Orange II removal was obtained. Langmuir isotherm and the pseudo-second-order kinetics provided the best correlation with the experimental data. Intra-particle diffusion model showed that adsorption process affected by external mass transfer and diffusion. The excellent adsorption efficiency and reusable performance suggested that CTAB-Al-Bent can act as an excellent adsorbent material for anionic dye wastewater treatment.

Keywords: CTAB-Al-Bent; Orange II; Adsorption isotherm; Kinetics; Adsorption mechanism

1. Introduction

With the rapid development of industry, the discharge of industrial wastewater increased year by year and environment pollution problem caught more and more attention. As one of the industrial pollutants, most of printing and dyeing wastewater contained aromatic and azo compounds [1], with highly toxic and hard-degradable. Dyes are the main components in printing and dyeing effluent, affecting the aquatic life and the growth of microorganisms. Therefore, it is necessary to find appropriate treatment strategies for efficient removal of dyes from wastewater system before discharge.

Currently, there are many methods for the removal of dyes from aqueous solutions, such as adsorption, chemical oxidation, membrane processes and biological degradation [2–5]. Among them, adsorption is the most popular method due to its easy-operation, low cost, recyclable and high-efficiency in dealing with various pollutants [6].

Nowadays, many non-conventional low-cost adsorbents were employed, such as bamboo fibers [7], zeolite [8], and activated carbon [9]. Recently, due to their abundance, low price, and high specific surface area, bentonite has been used to remove various pollutants: organic pollutants [10,11], metal ions [12,13], and dyes [14,15]. However, its adsorption capacity toward anionic dye is very low due to its negative charged and hydrophilic surfaces [16]. Several routes have been employed to modify clays and clay minerals [17], such as ion exchange reactions with inorganic cations and organic cations, pillaring by different types of poly(hydroxo metal) cations, dehydroxylation and calcination, reaction with acids, grafting of organic compounds, and binding of inorganic and organic anions at the edges etc. Among them, hydroxy-aluminium cat-

*Corresponding author.

ions pillared interlayered clays [18] and alkylammonium ions exchange organo-montmorillonites are well-known [19–25] and have been identified as innovative and promising classes of adsorbent materials. However, extensive studies mainly focused on increasing the removal efficiency towards pollutants by different modifying ways. More detailed investigations on adsorption mechanisms of CTAB-Al-Bent towards dyes need to be explored.

Based on our previous work [26], CTAB-Al-Bent was synthesized and the batch adsorption experiments were carried out to investigate its adsorption property towards anionic dye Orange II (4-(2-hydroxy-1-naphthylazo) benzenesulfonic acid sodium), which is extensively used in textiles, paper, foodstuffs, hair and leather colouring [27]. The influence factors, contact time, temperature, initial concentration, pH and adsorbent dosages, on Orange II adsorption were systematically studied. Meanwhile, kinetics, adsorption isotherms, and thermodynamics were also investigated to explore the adsorption mechanism of Orange II onto the modified bentonite.

2. Materials and methods

2.1. Materials

Aluminium chloride ($AlCl_3$, A.R.), sodium hydroxide (NaOH, A.R.), cetyltrimethyl ammonium bromide ($C_{19}H_{42}BrN$, CTAB, A.R.), 4-(2-hydroxy-1-naphthylazo) benzene-sulfonic acid sodium ($C_{16}H_{11}N_2O_4SNa{\cdot}5H_2O$, Orange II, A.R.), ethyl alcohol (CH_3CH_2OH, A.R.) were obtained from Sinopharm Chemical Reagent Co., Ltd., and used without further purification. The raw bentonite was supplied by xinyang, Henan province. Triply distilled water was used in all experiments.

2.2. Preparation of various bentonite adsorbents

Before modification, the raw bentonite was purified: 100 g raw bentonite was added into 1000 mL distilled water with stirring at 800 rpm for 0.5 h at room temperature and then standing 20 min. The upper solution and lower residual were abandoned, and the obtained sample was dried in the oven at 333 K and grinded to powder, coded as pure bentonite (P-Bent).

Al-Bent and CTAB-Al-Bent were prepared according to the references reported [23,24,28]. Typically, to prepare the pristine hydroxy-aluminum solutions, 0.48 mol L^{-1} NaOH solution was slowly added into 0.2 mol L^{-1} $AlCl_3$ solution under vigorous stirring at 353 K, until the OH^-/Al^{3+} molar ratio reached 2.4, then stored at this temperature for 24 h. Then P-Bent was introduced with 10 mmol Al/g bentonite and the slurry was stirred at 333 K for 24 h. The obtained products were washed several times with distilled water, dried at 333 K, activated for 1 h at 413 K, grinded to powder and kept in a desiccator for further use, coded as Al-Bent.

CTAB-Bent and CTAB-Al-Bent were prepared with the amount of CTAB equivalent to 100% of cation exchange capacity (CEC) of Bent or Al-Bent and vigorous stirring for 2 h at 343 K. The products were collected by centrifugation and dried at 333 K, grinded to powder and kept in a desiccator for further use.

2.3. Adsorbent characterization techniques

The X-ray diffraction (XRD) patterns of the samples were measured with Rigaku Corporation XRD/Max2550VB+/PC and recorded in the range of 2–80° with a scanning rate of 0.02° s^{-1} and desktop scanning electron microscope (SEM, TM3030, Hitachi Limited) was used to study their surface morphology. The elemental compositions were determined by means of energy dispersive spectroscopy (EDX, high vacuum, Quanta 200, FEI Corporation).

The Fourier transformed infrared spectroscopy (FTIR, Tensor27, BRUKER, Germany) were performed in the range of 4000–400 cm^{-1} with KBr pellets.

2.4. Adsorption behavior

A certain amount of adsorbent was added into 25 mL Orange II solution at definite concentration with stirring for a certain time at certain temperature. After adsorption the adsorbent was separated by centrifuge at 8000 rpm for 10 min, and the supernatant was filtered through a 0.45 um membrane filter. The residual concentration of Orange II was determined at maximum absorbance wavelength (485 nm) with UV-vis spectroscopy (UVT6, Beijing Purkinje General Instrument Co. Ltd, China).

The removal (%) and adsorption amount (q_t) can be calculated according to Eqs. (1) and (2):

$$Removal(\%) = \frac{C_0 - C_t}{C_0} \times 100\% \quad (1)$$

$$q_t = \frac{(C_0 - C_t)V}{W} \quad (2)$$

where C_0 and C_t are the respective Orange II concentration (mg L^{-1}) in solution at initial time, and at time t. q_t is the amount (mg g^{-1}) of Orange II adsorbed onto the adsorbent at time t. V is the volume of Orange II solution (mL) and W is the dry weight of the adsorbent (mg).

2.5. Desorption and recycle of CTAB-Al-Bent

0.02 g CTAB-Al-Bent was immersed into 50 mL Orange II aqueous solution (50 mg L^{-1}). When the adsorption equilibrium was reached, CTAB-Al-Bent was separated by centrifuge and then put into 50 mL of CH_3CH_2OH as desorption solution. The Orange II concentration was also analyzed and the desorption ratio (D%) calculated as Eq. (3):

$$D(\%) = \frac{C_d V_d}{(C_0 - C_e)V_i} \times 100\% \quad (3)$$

where C_0 and C_e are concentration (mg L^{-1}) of Orange II in solution at initial time and equilibrium time, respectively. C_d is the concentration of Orange II in the desorption solution (mg L^{-1}). V_i and V_d are the volume of the adsorption solution and the desorption solution (mL), respectively. After desorption, the recovered adsorbent was separated by centrifuge, washed several times by distilled water and then immersed into the dye solution again for reuse.

3. Results and discussion

3.1. Adsorbent characterization

3.1.1. X-ray diffraction (XRD)

The XRD patterns of various bentonites are shown in Fig. 1a. For P-Bent, the main compensating cations were calcium and magnesium, which was in agreement with the observed d_{001} distance of 13.35 Å. After pillaring by hydroxy-aluminum cations, d_{001} value increased to 15.33 Å (Al-Bent). The interlayer spacing distance of Al-Bent (0.57 nm) was lower than the size (~0.9 nm) of hydroxyl-aluminum polycations ($[AlO_4Al_{12}(OH)_{24}(OH_2)_{12}]^{7+}$) [21,29], indicating only hydroxy-aluminum cations entered into the interlayer. When ion exchanged bentonite with CTAB cation (CTAB-Bent), d_{001} value increased to 17.34 Å. For CTAB-Al-Bent, d_{001} value of 17.66 Å was obtained, a little larger than that of CTAB-Bent. This implies that the basal space of the resultant composites depend on the surfactant and hydroxy-aluminum cations. From the EDX elemental analysis results (Table 1), the Al/Si ratio of CTAB-Al-Bent (0.29) was lower than that of Al-Bent (0.47), indicating that there is an ion exchange between the intercalated surfactant cations and the hydroxy-aluminum cations [30].

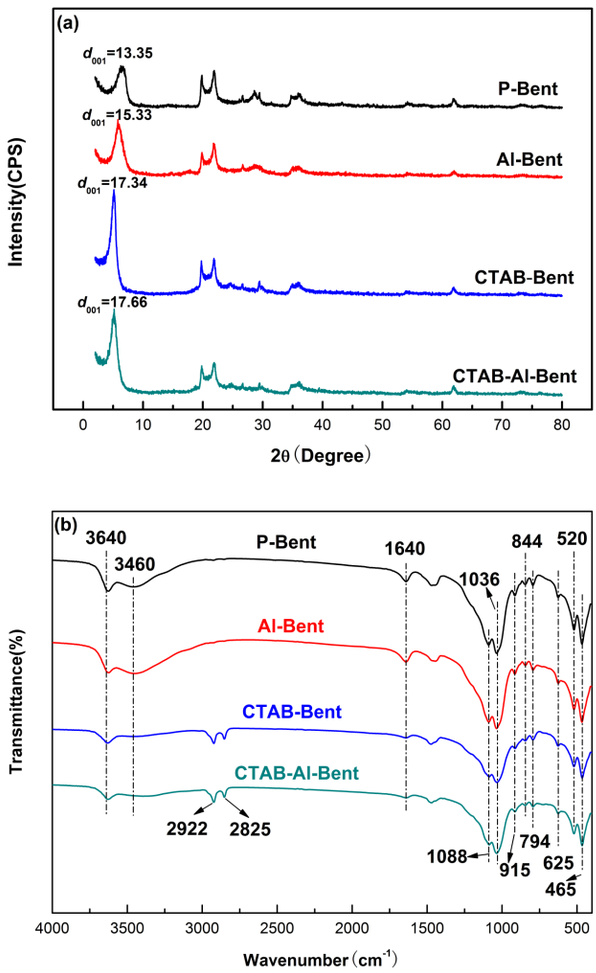

Fig. 1. XRD patterns (a) and FTIR spectra (b) of P-Bent, Al -Bent, CTAB- Bent and CTAB-Al-Bent.

3.1.2. FTIR spectra

FTIR spectroscopy is a sensitive technique to probe the interaction type, configuration and local environment of the surfactant cations in the interlamellar region of clay [31]. The comparative FTIR spectra of P-Bent, Al-Bent, CTAB-Bent and CTAB-Al-Bent are shown in Fig. 1b. The band at 3640 cm^{-1} assigned to stretching vibrations of structural OH groups [32], whereas the bands at 3460 and 1640 cm^{-1} can be assigned to the O-H deformation of water [33–35]. The Si-O stretching (longitudinal and transverse mode) vibrations were observed at 1088 and 1036 cm^{-1}, respectively [31]. In the spectra of P-Bent, the band at 915 cm^{-1} can be assigned to the deformation of Al-Al-OH in the octahedral layers [35,36]. Coupled Al-O/Si-O appeared at 844 cm^{-1}, 794 cm^{-1}, 625 cm^{-1} and Al-O-Si deformations appeared at 520 cm^{-1}, 465 cm^{-1} [31], indicating the existence of the essential structure of bentonite [31,32].

In FTIR spectra of Al-Bent, a considerable increase in the intensities of the bands at 3460 and 1640 cm^{-1} of sorbed water molecules, due to the introduction of hydroxy-aluminum cations increasing large amounts of water and hydroxyl. However, a considerable decrease in the intensities of these two bands when CTA^+ cations were introduced [31,37]. As a result, the amount of water in the interlayer region reduced and the surface properties of bentonite changed from natural hydrophilic to organophilic character, which was consistent with the reference reported [31]. It can also be found that the new peaks at 2922 and 2852 cm^{-1} corresponded to the C-H asymmetric and symmetric stretching vibrations of cetyl chain, respectively [38]. In addition, the banding vibration of $–CH_3$ was observed at 1474 cm^{-1} in organic intercalator [25].

3.2. Factors affecting the removal efficiency of Orange II

3.2.1. Effect of various bentonite adsorbents

The type of adsorbents affects the removal of Orange II. From Fig. 2, only 8.60% Orange II was removed by P-Bent, 12.56% and 56.61% removal were obtained for Al-Bent and CTAB-Bent, respectively. While 78.18% removal was observed for CTAB-Al-Bent, moreover, CTAB-Al-Bent can be separated from the solution more easily, indicating the introduction of organic cation changed the clay from hydrophilic to hydrophobic form [39]. So, CTAB-Al-Bent was selected in the further study.

Table 1
EDX results of CTAB and Al modified bentonite

Samples	Al (wt.%)	Si (wt.%)	Ca (wt.%)	Al/Si (wt.%)
P-Bent	6.62	36.42	0.18	0.18
Al-Bent	9.70	20.79	–	0.47
CTAB-Al-Bent	5.82	19.78	–	0.29

3.2.2. Effect of contact time and temperature

The effect of contact time and temperature on Orange II removal by CTAB-Al-Bent was studied and the results are shown in Fig. 3a. The Orange II removal initially increased with contact time prolonging and then gradually unchanged, reaching a maximum removal of approximately 82.09% at 30 min (303 K). So in the following experiments, 30 min was selected to ensure adsorption equilibrium.

The removal efficiency increased from about 78.18% to 82.09% with the temperature increased from 298 K to 303 K. This can be ascribed to faster mass transfer in the solution and higher collision frequency between the adsorbent and the dye molecules. However, the removal efficiency decreased with temperature increased further, indicating the adsorption of Orange II onto CTAB-Al-Bent was exothermic in nature [40], which was consistent with the references [37,41].

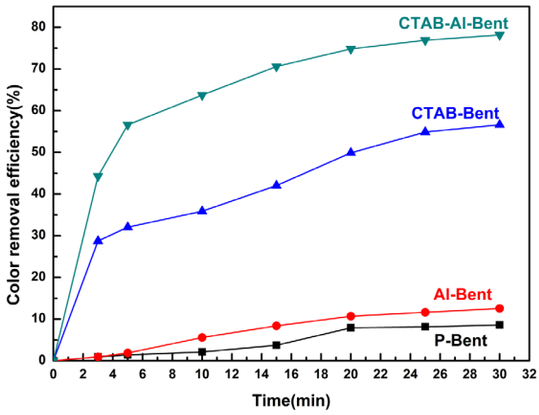

Fig. 2. Effect of different adsorbents on Orange II removal.

3.2.3. Effect of initial Orange II concentration

Fig. 3b presents the effect of initial Orange II concentration (50, 100, 150 and 200 mg L^{-1}) on the removal efficiency. The corresponding removal efficiencies after 30 min were 78.18, 62.59, 45.86, and 33.16%, for initial concentration at 50, 100, 150 and 200 mg L^{-1}, respectively. These results showed that changes in the Orange II initial concentration affected the removal process significantly. The increment in initial concentration of Orange II resulted in rapid initial removal within the first 15 min. This implied that at higher initial concentration the adsorption process was highly concentration controlled. Almost total removal of Orange II was achieved within 30 min for 50 mg L^{-1}, while 200 mg L^{-1} showed lowest removal efficiency, probably indicating insufficient active sites for Orange II adsorption [35,42].

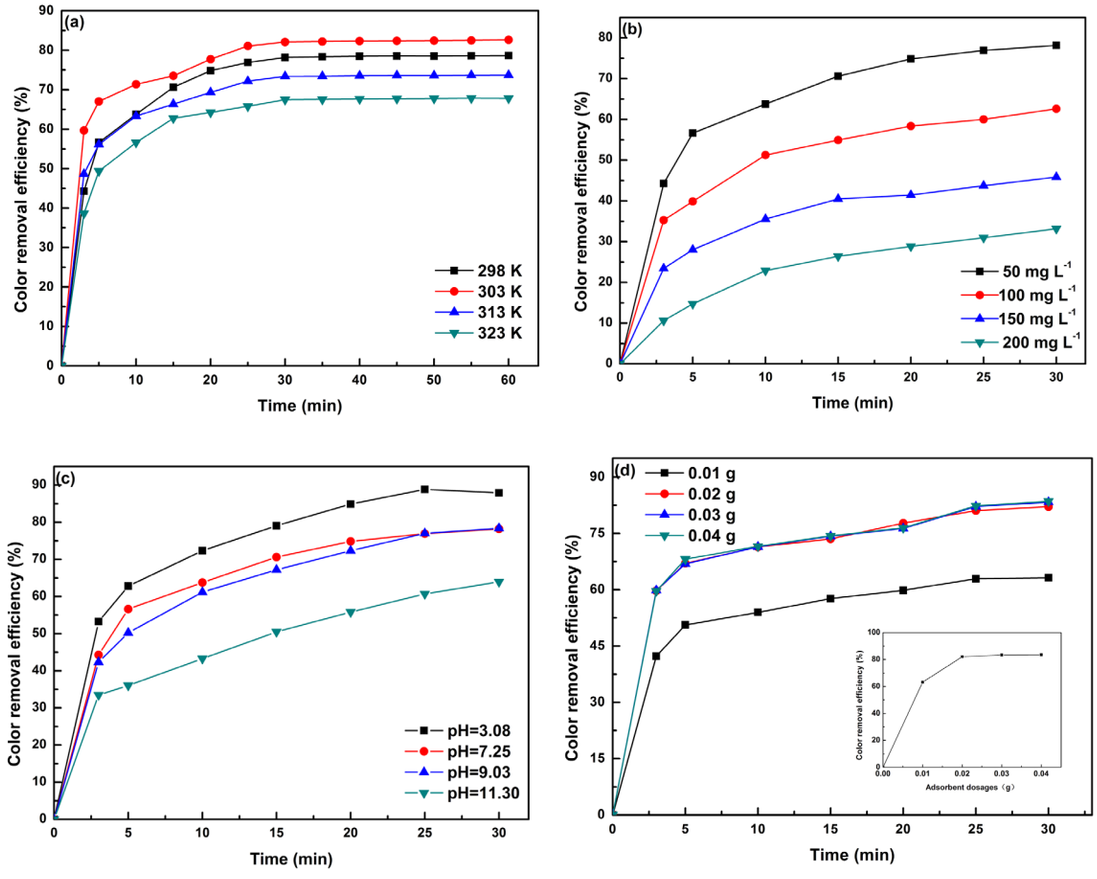

Fig. 3. Effect of various operating parameters on Orange II removal.

3.2.4. Effect of initial pH

In order to study the effect of pH on the adsorption capacity of CTAB-Al-Bent, the unadjusted pH of Orange II (7.25), acidic (3.08) and alkaline (9.03, 11.30) were tested (Fig. 3c). 88.84% removal efficiency at pH 3.08 was obtained, then decreased with pH increasing, and only 63.96% was observed at pH 11.30. It may be due to that pH affected the surface charge of the adsorbent and the degree of ionization of adsorbate [43]. At lower pH, the protonization of surface –OH groups to $–OH_2^+$ [43], consequently the positive sites increased, thereby electrostatic attraction enhanced between the positive charged adsorption sites and the negative charged dyes. In alkaline condition, on one hand, the protonation of surface –OH decreased and consequently the positive sites decreased; and on the other hand, the abundance of OH^- ions competing with the anionic dye for the adsorption sites, resulted in the reduction of exchangeable dye anions on the adsorbent [43]. Meanwhile, the anionic dye molecular predominated, the ionic electrostatic repulsion between the negatively charged bentonite surface and the anionic adsorbate also attributed to the decrease of the removal efficiency of dye [11].

3.2.5. Effect of adsorbent dosages

The effect of adsorbent dosages on Orange II removal is shown in Fig. 3d. The removal efficiency increased with the increasing amount of adsorbent CTAB-Al-Bent and 78.18% removal was observed when the dosage was 0.02 g, then gradually kept stable. Further increasing the dosage would increase the cost, so the dosage of 0.02 g in 50 mL 50 mg L^{-1} Orange II was applied in the further study.

3.3. Kinetics study

Two typical kinetic models, pseudo-first-order and pseudo-second-order equations are analyzed, which are expressed by Eqs. (4) and (5), respectively:

$$\ln(q_e - q_t) = \ln q_e - k_1 t \tag{4}$$

$$\frac{t}{q_t} = \frac{1}{k_2 q_e^2} + \frac{1}{q_e} t \tag{5}$$

where k_1 (min^{-1}) and k_2 (L^{-1} mg^{-1} min^{-1}) are the pseudo-first-order and pseudo-second-order rate constants, respectively, q_e (mg g^{-1}) and q_t (mg g^{-1}) are the adsorption amounts of Orange II at equilibrium contact time and t min, respectively. A comparison of the results with the fitting line is plotted in Fig. 4 and the kinetic parameters are summarized in Table 2.

It was observed that the correlation coefficients (R^2) of pseudo-second-order model were higher than that of pseudo-first-order model, and $q_{e,2}$ values calculated were close to

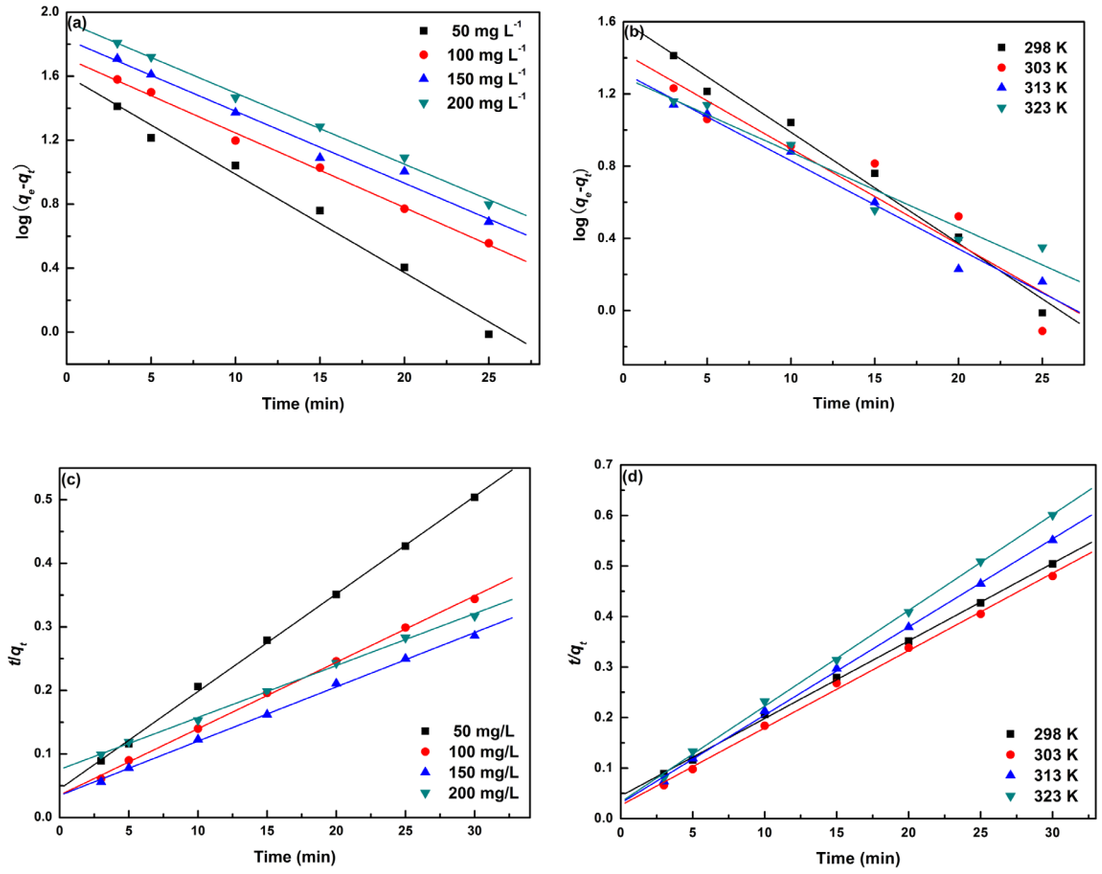

Fig. 4. The pseudo-first-order (a, b) and pseudo-second-order kinetics (c, d) for Orange II adsorption onto CTAB-Al-Bent.

Table 2
The kinetic parameters for Orange II adsorption onto CTAB-Al-Bent

T(K)	C_0 (mg L^{-1})	$q_{e,exp}$ (mg g^{-1})	Pseudo-first-order model			Pseudo-second-order model		
			q_{1e} (mg g^{-1})	k_1 (min^{-1})	R_1^2	q_{2e} (mg g^{-1})	k_2 (L mg^{-1} min^{-1})	R_2^2
298	50	59.52	40.10	0.1417	0.9920	65.15	0.0052	0.9996
	100	87.21	51.55	0.1074	0.9980	95.60	0.0031	0.9994
	150	104.90	67.63	0.1034	0.9931	117.10	0.0021	0.9991
	200	94.64	87.08	0.1024	0.9977	122.25	0.0009	0.9992
303	50	62.50	26.73	0.1220	0.9486	65.32	0.0089	0.9989
313	50	55.87	20.74	0.1122	0.9886	57.37	0.0099	0.9995
323	50	51.37	19.67	0.0959	0.9763	52.74	0.0109	0.9995

$q_{e,exp}$, indicating this adsorption process could be described better by the pseudo-second-order model.

Activation energy (E_a) can be calculated from the Arrhenius equation:

$$\ln k = \ln A - \frac{E_a}{RT} \tag{6}$$

where E_a (KJ mol^{-1}) is the apparent adsorption energy; k is reaction rate constant; R (8.314 J mol^{-1} K^{-1}) and T (K) are ideal gas constant and thermodynamic temperature, respectively. Here the calculated E_a value was 19.38 kJ mol^{-1}, indicating that the lower potential barriers of the adsorption process [44].

The intra-particle diffusion model, described by Eq. (7), considers the mass transfer inside the adsorbent particle as the prevalent step of the process [45].

$$q_t = k_{id} t^{0.5} + C \tag{7}$$

where K_{id} (mg g^{-1} min$^{-0.5}$) is the intra-particle diffusion rate constant and C (mg g^{-1}) represents the boundary layer thickness. If C = 0, diffusion is limited in the process of adsorption rate; C > 0, external mass transfer and diffusion are within the limit rate of adsorption process [46]. The plotting of q versus $t^{0.5}$ for the intra-particle stage provided the values of both parameters (Fig. 5). It can be found that the fitting curve was piecewise, without forming a good linear straight line, indicating adsorption was not a simple internal diffusion process. C values were all positive, indicating adsorption process affected by external mass transfer and diffusion.

3.4. Adsorption isotherms

In this study, Langmuir, Freundlich and Temkin isotherms were used and expressed by Eqs. (8), (9) and (10), respectively:

$$\frac{C_e}{q_e} = \frac{1}{K_L q_m} + \frac{C_e}{q_m} \tag{8}$$

$$\ln q_e = \ln K_F + \frac{1}{n} \ln C_e \tag{9}$$

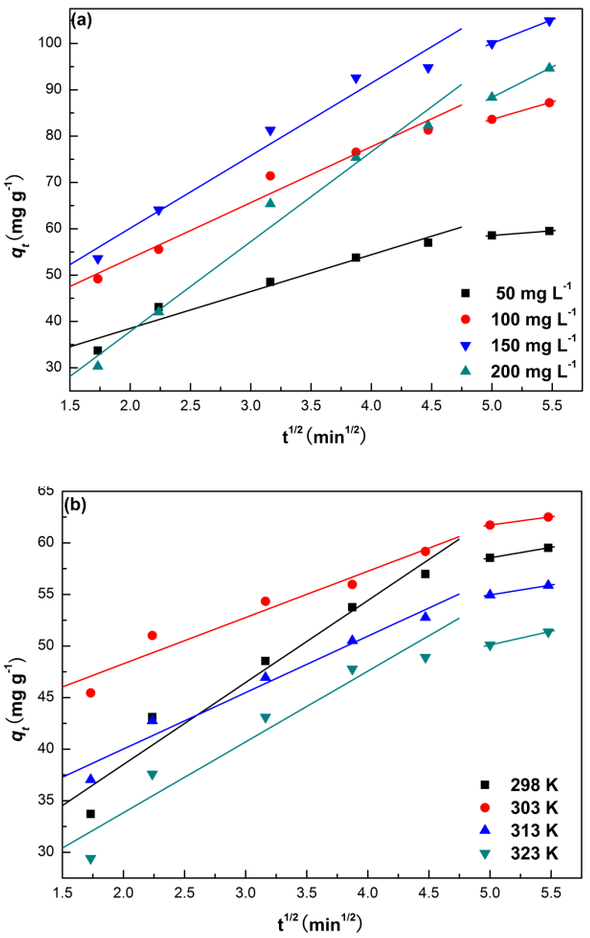

Fig. 5. The intra-particle diffusion model for Orange II adsorption onto CTAB-Al-Bent at various concentrations (a) and temperatures (b).

$$q_e = A + B \ln C_e \tag{10}$$

where q_e (mg g^{-1}) and q_m (mg g^{-1}) are the equilibrium adsorption amount of adsorbate and the monolayer saturation adsorption amount on the adsorbent, respectively. C_e (mg L^{-1})

is the equilibrium concentration of adsorbate. The K_L and K_F are the Langmuir and Freundlich isotherm constant, respectively. And n is heterogeneity factor used to describe adsorption intensity of the adsorbent. A (L g^{-1}) is the Temkin constant. B = RT/β, where β (J mol^{-1}) is the adsorption heat constant.

The fitting lines are plotted in Fig. 6 and the isotherm parameters are summarized in Table 3. The correlation coefficients (R^2) of Langmuir isotherm were higher than that of Freundlich and Temkin isotherms, and the monolayer saturation adsorption amount (q_m) was close to the calculated value ($q_{e,max}$), indicating that the Langmuir isotherm fitted the best to the experimental data, and the monolayer coverage nature of the adsorbate on the surface of CTAB-Al-Bent [47].

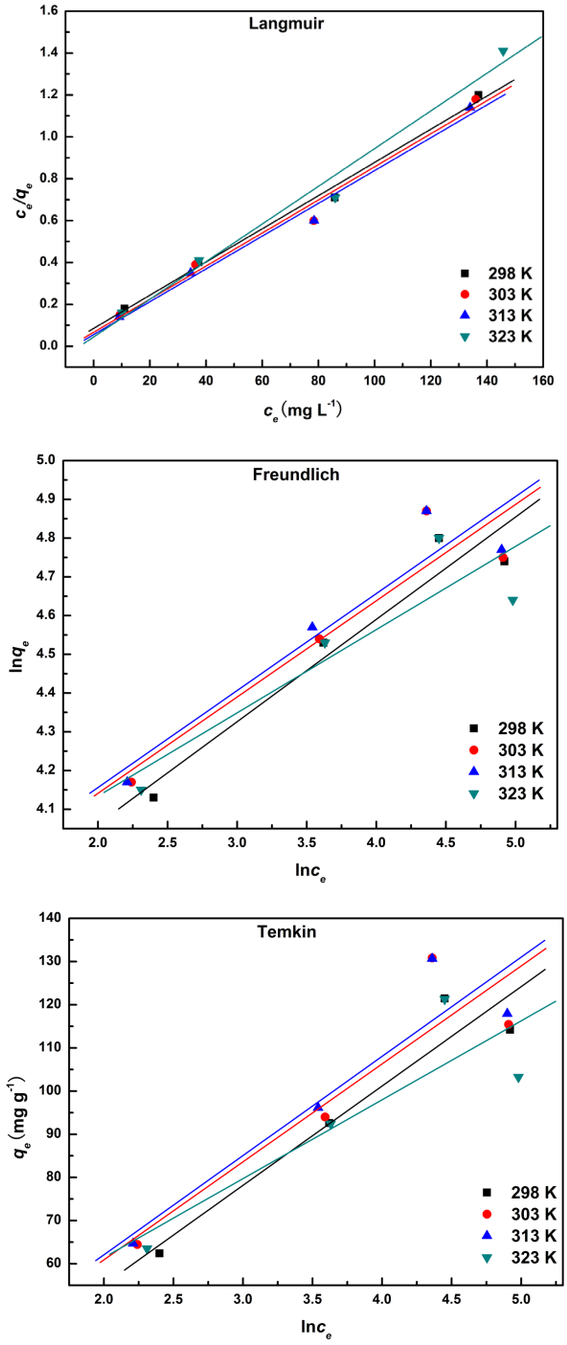

Fig. 6. Langmuir, Freundlich and Temkin isotherm for Orange II adsorption onto CTAB-Al-Bent.

Table 4 shows the maximum adsorption capacity ($q_{m,max}$) for various adsorbents towards Orange II at room temperature. As can be seen, higher $q_{m,max}$ was obtained for CTAB-Al-Bent than most of the reported adsorbents, except activated carbon and zirconium-based chitosan microcomposite. However, the low cost and the simple synthesis procedure suggested the potential application of CTAB-Al-Bent adsorbent in anionic dye wastewater treatment.

3.5. Thermodynamics study

The thermodynamic parameters like adsorption free energy change (ΔG_0), entropy change (ΔS_0), enthalpy change (ΔH_0) can be calculated by Eqs. (11)–(13), respectively:

$$\ln K_c = -\frac{\Delta H_0}{RT} + \frac{\Delta S_0}{R} \tag{11}$$

Table 3
The isotherm parameters for Orange II adsorption onto CTAB-Al-Bent

Model	Parameters	T (K)			
		298	303	313	323
Langmuir	q_m (mg g^{-1})	126.10	126.42	127.55	111.11
	K_L (L mg^{-1})	0.0932	0.1193	0.1408	0.2043
	r^2	0.9963	0.9912	0.9938	0.9908
Freundlich	n	3.786	4.024	3.995	4.655
	K_F	34.248	38.255	38.698	40.630
	r^2	0.9630	0.9374	0.9404	0.9034
Temkin	A	9.090	15.522	16.125	24.869
	B	23.021	22.692	22.979	18.279
	r^2	0.9892	0.9131	0.9318	0.8782

Table 4
The maximum adsorption capacity ($q_{e,max}$) for various adsorbents

Adsorbents	$q_{m,max}$ (mg g^{-1})	References
CTAB-Al-Bent	126.10 (289K)	This paper
1-butanol-TiO_2	19.972	[48]
2-butanol-TiO_2	24.327	
CTAB-zeolite	38.96	[49]
OTAB-palygorskites	92	[27]
DDAB-palygorskites	88	
MTPB-Bent	53.78	[44]
n-HTPB-Bent	33.79	
Activated carbon	404	[50]
Zr-chitosan microcomposite	926	[51]

$$K_c = \frac{q_e}{C_e} \tag{12}$$

$$\Delta G_0 = \Delta H_0 - T\Delta S_0 \tag{13}$$

where K_c is the equilibrium constant, R (8.314 J mol^{-1} K^{-1}) and T (K) are ideal gas constant and thermodynamic temperature, respectively.

The thermodynamic parameters are summarized in Table 5. The negative ΔG_0 and ΔH_0 indicated the adsorption was spontaneous and exothermic, the rise of temperature was not conducive to the adsorption process, which was consistent with the experimental results. And positive ΔS_0 showed that the adsorption was entropy increase process.

3.6. Desorption and recycle of the CTAB-Al-Bent

Fig. 7a shows Orange II desorption in ethyl alcohol. Over 95.74% of Orange II desorbed within 30 min, indicating the high desorption capacities of CTAB-Al-Bent. It was demonstrated that CTAB-Al-Bent exhibited a good reversibility for the adsorption and desorption of Orange II, also suggesting the physical character of the interaction between CTAB-Al-Bent and Orange II.

The regenerated CTAB-Al-Bent adsorbent was also investigated by successively performing the adsorption-desorption cycles (Fig. 7b). The removal efficiency of Orange II decreased slightly from 78.18% to 74.72% after five cycles, indicating the excellent reusable performance of CTAB-Al-Bent and its potential application in anionic dye wastewater treatment.

3.7. Identification of the possible adsorption mechanism

The structural characteristics of the prepared adsorbents and their adsorption performance are shown in Table 6. Higher specific surface area and interlayer space (d_{001}) for Al-Bent correspond to a little increase in Orange II removal, while significantly increase in Orange II removal and interlayer space (d_{001}) were observed after CTAB modification, meanwhile the specific surface area decreased, indicating surface area was not the most important factor during the adsorption process. Fig. 1b shows a considerable decrease in the intensities at 3460 and 1640 cm^{-1} when CTA$^+$ cation was introduced, indicating the organophilic character of the bentonite surface, which was benefit for the adsorption. The removal efficiency increased at acidic condition (Fig. 3c), indicating the electrostatic attraction involved in the adsorption process.

To further investigate the adsorption mechanism, spent CTAB-Al-Bent was also characterized by FTIR spectra (Fig. 8). The intensities of the bands at 3460 and 1640 cm^{-1} of sorbed water molecules decreased after adsorption, indicating that the hydroxyl surface groups maybe partly replaced by the adsorbate.

In addition, CTAB-Al-Bent exhibited substantially enhanced adsorption capacities toward Orange II, maybe attribute to the interaction of the organic solutes into the organic solvent-like hydrophobic phase created by the alkyl

Table 5
Thermodynamic parameters for Orange II adsorption onto CTAB-Al-Bent

T (K)	K_c	ΔG_0 (kJ mol^{-1})	ΔH_0 (kJ mol^{-1})	ΔS_0 (J mol^{-1}K^{-1})
303	4.58	–3.83	–33.02	96.50
313	2.76	–2.65		
323	2.07	–1.96		

Table 6
The structural characteristics of the prepared adsorbents and their adsorption performance

Sorbent	BET surface area (m^2 g^{-1})	d_{001} (Å)	Removal (%)
P-Bent	25.46	13.35	8.60
Al-Bent	36.05	15.33	12.56
CTAB-Al-Bent	12.83	17.66	78.18
Spent CTAB-Al-Bent	14.25	18.15	74.72–78.18

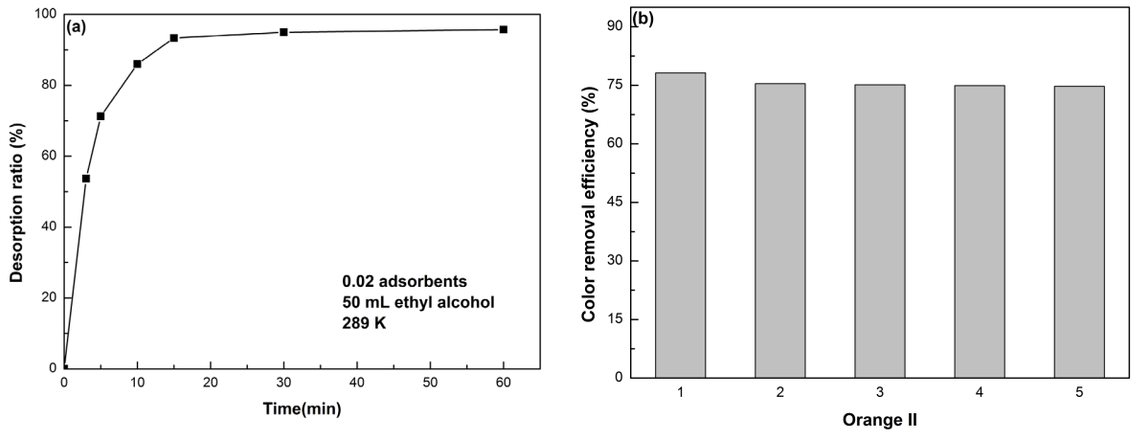

Fig. 7. Desorption ratio of Orange II (a) and reuse of adsorbents for Orange II (b).

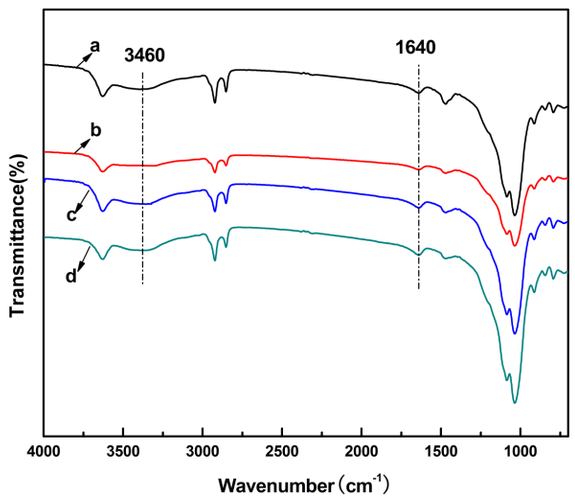

Fig. 8. FTIR spectra of CTAB-Al-Bent before (a) and after adsorption at various pH values (pH = 3.08 (b); pH = 7.25 (c) and pH = 9.03 (d)).

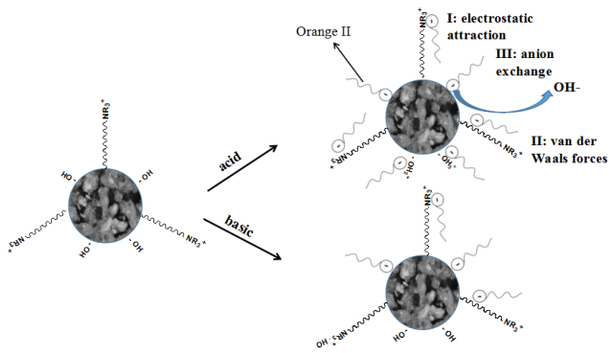

Fig. 9. Possible adsorption mechanism of Orange II onto CTAB-Al-Bent.

chains of the surfactant, which was typical of the van der Waals interactions [52].

Based on the above discussions, the possible adsorption mechanisms are proposed in Fig. 9. Adsorption of Orange II onto CTAB-Al-Bent maybe controlled by: (a) electrostatic attraction between CTAB-Al-Bent and the oppositely charged adsorbate; (b) van der Waals forces between Orange II molecules and alkyl chains of the surfactant and (c) anion exchange occurred between OH^- and negative charged Orange II.

4. Conclusion

An eco-friendly and low-cost adsorbent CTAB-Al-Bent was prepared successfully and used for Orange II removal from water. Batch studies were performed to examine the adsorption capability and the regeneration of adsorbent. Compared with P-Bent and Al-Bent, CTAB-Al-Bent exhibited higher adsorption capacity for Orange II removal. The removal efficiency decreased with pH increasing, indicating that the surface charge on CTAB-Al-Bent played a vital role in adsorption process. And the process can be described well by the pseudo-second-order kinetic and the Langmuir isotherm model. A possible adsorption mechanism based on electrostatic attraction, van der Waals forces and anion exchange was proposed. The results revealed that CTAB-Al-Bent can be acted as a low-cost, effective, and reusable potential adsorbent applied in anionic dye removal from effluent.

References

[1] Y. Fan, H.J. Liu, Y. Zhang, Y. Chen, Adsorption of anionic MO or cationic MB from MO/MB mixture using polyacrylonitrile fiber hydrothermally treated with hyper-branched polyethylenimine, J. Hazard. Mater., 283 (2015) 321–328.
[2] S.J. You, D.H. Tseng, J.Y. Deng, Using combined membrane processes for textile dyeing wastewater reclamation, Desalination, 234 (2008) 426–432.
[3] L. Zheng, X.J. Wang, X.Z. Wang, Reuse of reverse osmosis concentrate in textile and dyeing industry by combined process of persulfate oxidation and lime-soda softening, J. Clean. Prod., 108 (2015) 525–533.
[4] B.M. Esteves, S.D. Rodrigues, R.A.R. Boaventura, F.J. Maldonado-Hodar, L.M. Madeira, Coupling of acrylic dyeing wastewater treatment by heterogeneous Fenton oxidation in a continuous stirred tank reactor with biological degradation in a sequential batch reactor, J. Environ. Manage., 166 (2016) 193–203.
[5] V. Suba, G. Rathika, Novel Adsorbents for the removal of dyes and metals from aqueous solution—A Review, J. Adv. Phys., 5 (2016) 277–294.
[6] M. Alkan, M. Doğan, Y. Turhan, Ö. Demirbaş, P. Turan, Adsorption kinetics and mechanism of maxilon blue 5G dye on sepiolite from aqueous solutions, J. Chem. Eng., 139 (2008) 213–223.
[7] S. Sribenja, S. Saikrasun, Adsorption behavior and kinetics of Lac dyeing on poly(ethyleneimine)-treated bamboo fibers, Fiber. Polym., 16 (2015) 2391–2400.
[8] E. Alver, A.Ü. Metin, Anionic dye removal from aqueous solutions using modified zeolite: Adsorption kinetics and isotherm studies, J. Chem. Eng., 200–202 (2012) 59–67.
[9] H. Trevino-Cordero, L.G. Juárez-Aguilar, D.I. Mendoza-Castilloa, V. Hernández-Montoya, A. Bonilla-Petriciolet, M.A. Montes-Moránb, Synthesis and adsorption properties of activated carbons from biomass of Prunusdomestica and Jacaranda mimosifolia for the removal of heavy metals and dyes from water, Ind. Crop. Prod., 42 (2013) 315–323.
[10] A. Khenifi, B. Zohra, B. Kahina, H. Houari, D. Zoubir, Removal of 2, 4-DCP from wastewater by CTAB/bentonite using one-step and two-step methods: A comparative study, Chem. Eng. J., 146 (2009) 345–354.
[11] X.D. Xin, W. Si, Z.X. Yao, R. Feng, B. Du, L.G. Yan, Q. Wei, Adsorption of benzoic acid from aqueous solution by three kinds of modified bentonites, J. Colloid Interf. Sci., 359 (2011) 499–504.
[12] C. Volzone, L.B. Garrido, Use of modified hydroxy-aluminum bentonites for chromium(III) removal from solutions, J. Environ. Manage., 88 (2008) 1640–1648.
[13] E. Orucoglu, S. Haciyakupoglu, Bentonite modification with hexadecylpyridinium and aluminumpolyoxy cations and its effectiveness in Se(IV) removal, J. Environ. Manage., 160 (2015) 30–38.
[14] B. Benguella, A. Yacouta-Nour, Adsorption of Bezanyl Red and Nylomine Green from aqueous solutions by natural and acid-activated bentonite, Desalination, 235 (2009) 276–292.
[15] Q. Kang, W.Z. Zhou, Q. Li, B.Y. Gao, J.X. Fan, D.Z.Shen, Adsorption of anionic dyes on poly(epicholorohydrin dimethylamine) modified bentonite in single and mixed dye solutions, Appl. Clay Sci., 45 (2009) 280–287.

[16] A.S. Özcan, B. Erdem, A. Özcan, Adsorption of Acid Blue 193 from aqueous solutions onto Na-bentonite and DTMA-bentonite, J. Colloid Interf. Sci., 280 (2004) 44–54.
[17] L.B.D. Paiva, A.R. Morales, F.R.V. Díaz, Organoclays: Properties, preparation and applications, Appl. Clay Sci., 42 (2008) 8–24.
[18] Z. Bouberkaa, S. Kachab, M. Kamechea, S. Elmalehc, Z. Derrichea, Sorption study of an acid dye from an aqueous solutions using modified clays, J. Hazard. Mater., B119 (2005) 117–124.
[19] H. Zaghouane-Boudiaf, M. Boutahala, S. Sahnoun, C. Tiar, F. Gomri, Adsorption characteristics, isotherm, kinetics, and diffusion of modified natural bentonite for removing the 2,4,5-trichlorophenol, Appl. Clay Sci., 90 (2014) 81–87.
[20] N. Liu, M.X. Wang, M.M. Liu, F. Liu, L. Weng, L.K. Koopal, W.F. Tan, Sorption of tetracycline on organo-montmorillonites, J. Hazard. Mater., 225–226 (2012) 28–35.
[21] L.Y. Ma, Q. Zhou, T. Li, Q. Tao, J.Y. Zhu, P. Yuan, R.L. Zhu, H.P. He, Investigation of structure and thermal stability of surfactant-modified Al-pillared montmorillonite, J. Therm. Anal. Calorim., 115 (2014) 219–225.
[22] M.E. Paroloa, G.R. Pettinaria, T.B. Mussoa, M.P. Sánchez-Izquierdob, L.G. Fernándezb, Characterization of organo-modified bentonite sorbents: The effect of modification conditions on adsorption performance, Appl. Surf. Sci., 320 (2014) 356–363.
[23] R.L. Zhu, L.Z. Zhu, J.X. Zhu, F. Ge, T. Wang, Sorption of naphthalene and phosphate to the CTMAB–Al_{13} intercalated bentonites, J. Hazard. Mater., 168 (2009b) 1590–1594.
[24] L.G. Yan, Y.Y. Xu, H.Q. Yu, X.D. Xin, Q. Wei, B. Du, Adsorption of phosphate from aqueous solution by hydroxy-aluminum, hydroxy-iron and hydroxy-iron-aluminum pillared bentonites, J. Hazard. Mater., 179 (2010) 244–250.
[25] L.G. Yan, L.L. Qin, H.A. Yu, S. Li, R.R. Shan, B. Du, Adsorption of acid dyes from aqueous solution by CTMAB modified bentonite: Kinetic and isotherm modeling, J. Mol. Liq., 211 (2015) 1074–1081.
[26] J. Wang, H.Z. Ma, W.F. Yuan, W.Y. He, S.S. Wang, J. You, Synthesis and characterization of an inorganic/organic-modified bentonite and its application in methyl orange water treatment, Desal. Water Treat., 52 (2014) 660–7672.
[27] B. Sarkar, Y.F. Xi, M. Megharaj, R. Naidu, Orange II adsorption on palygorskites modified with alkyl trimethylammonium and dialkyl dimethylammonium bromide -An isothermal and kinetic study, Appl. Surf. Sci., 51 (2011) 370–374.
[28] R.L. Zhu, T. Wang, F. Ge, W.X. Chen, Z.M. You, Intercalation of both CTMAB and Al_{13} into montmorillonite, J. Colloid. Interf. Sci., 335 (2009a) 77–83.
[29] Z.H. Qin, P. Yuan, J.Z. Zhu, H.P. He, D. Liu, S.Q. Yang, Influences of thermal pretreatment temperature and solvent on the organosilane modification of Al_{13}-intercalated/Al-pillared montmorillonite, Appl. Clay Sci., 50 (2010) 546–553.
[30] W.H. Xue, H.P. He, J.X. Zhu, P. Yuan, FTIR investigation of CTAB-Al-montmorillonite complexes, Spectro. Acta Part A., 67 (2007) 1030–1036.
[31] B. Caglar, C. Topcu, F. Coldur, G. Sarp, S. Caglar, A. Tabak, E. Sahin, Structural, thermal, morphological and surface charge properties of dodecyltrimethy lammonium-smectite composites, J. Mol. Struct., 1105 (2016) 70–79.
[32] Z.P. Tomić, D.P. Ašanin, R. Durović-pejčev, A. Dordevic, P. Makreski, Adsorption of acetochlor herbicide on inorganic- and organic-modified bentonite monitored by mid-infrared spectroscopy and batch adsorption, Spectrosc. Lett., 48 (2015) 685–690.
[33] F. Adam, J. Andas, I.A. Rahman, A study on the oxidation of phenol by heterogeneous iron silica catalyst, J. Chem. Eng., 165 (2010) 658–667.
[34] S.F. Zuo, R.X. Zhou, C.Z. Qi, Synthesis and characterization of aluminum and Al/REE pillared clays and supported palladium catalysts for benzene oxidation, J. Rare Earth, 29 (2011) 52–57.
[35] O.B. Ayodele, B.H. Hameed, Synthesis of copper pillared bentonite ferrioxalate catalyst for degradation of 4-nitrophenol in visible light assisted Fenton process, J. Ind. Eng. Chem., 19 (2013) 966–974.
[36] V.C. Farmer, J.D. Russel, The infra-red spectra of layer silicates, Spectrochim. Acta, 20 (1964) 1149–1173.
[37] L.G. Yan, J. Wang, H.A. Yu, Adsorption of benzoic acid by CTAB exchanged montmorillonite, J. Appl. Clay Sci., 37 (2007) 226–230.
[38] L. Wang, A.Q. Wang, Adsorption properties of Congo Red from aqueous solution onto surfactant-modified montmorillonite, J. Hazard. Mater., 160 (2008) 173–180.
[39] P. Baskaralingam, M. Pulikesi, D. Elango, V. Ramamurthi, S. Sivanesan, Adsorption of acid dye onto organbentonite, J. Hazard. Mater., 128 (2006) 138–144.
[40] Ö. Gök, A.S. Özcan, A. Özcan, Adsorption behavior of a textile dye of Reactive Blue 19 from aqueous solutions onto modified bentonite, Appl. Surf. Sci., 256 (2010) 5439–5443.
[41] Q. Zhou, R.L. Frost, H.P. He, Y.F. Xi, Changes in the surfaces of adsorbed para-nitrophenol on HDTMA organoclay—The XRD and TG study, J. Colloid Interf. Sci., 307 (2007) 50–55.
[42] R. Achma, A. Ghorbel, A. Dafinov, F. Medina, Copper-supported pillared clay catalysts for the wet hydrogen peroxide catalytic oxidation of model pollutant tyrosol, Appl. Catal. A., 349 (2008) 20–28.
[43] V. Vadivelan, K.K. Vasanth, Equilibrium, kinetic, mechanism, and process design for the sorption of methylence blue onto rice husk, J. Colloid Interf. Sci., 286 (2005) 90–100.
[44] S. Bouzid, A. Khenifi, K.A. Bennabou, R. Trujillano, M.A. Vicente, Z. Derriche, Removal of Orange II by Phosphonium-modified Algerian Bentonites, Chem. Eng. Commun., 202 (2015) 520–533.
[45] W.J. Weber, J.C. Morris, Kinetics of adsorption on carbon from solution, J. Sanit. Eng. Div. Am. Soc. Civ. Eng., 1 (1963) 1–2.
[46] A. Ronbanchob, P. Prasert, Batch and column studies of biosorption of heavy metal by Caulerpa lentillifera, J. Bioresource Technol., 99 (2008) 2766–2777.
[47] S. Karaca, A. Gürses, M. Açıkyıldız, M. Ejder (Korucu), Adsorption of cationic dye from aqueous solutions by activated carbon. Micropor. Mesopor. Mat., 115 (2008) 376–382.
[48] S. Jafari, B. Tryba, E. Kusiak-Nejman, J. Kapica-Kozar, A.W. Morawski, M. Sillanpää, The role of adsorption in the photocatalytic decomposition of Orange II on carbon-modified TiO_2, J. Mol. Liq., 220 (2016) 504–512.
[49] X.Y. Jin, B. Yu, Z.L. Chen, J.M. Arocena, R.W. Thring, Adsorption of Orange II dye in aqueous solution onto surfactant-coated zeolite: Characterization, kinetic and thermodynamic studies, J. Colloid Interf. Sci., 435 (2014) 15–20.
[50] G.S. Zhang, J.H. Qu, H.J. Liu, A.T. Cooper, R.C. Wu, $CuFe_2O_4$/activated carbon composite: A novel magnetic adsorbent for the removal of acid orange II and catalytic regeneration, Chemosphere, 68 (2007) 1058–1066.
[51] L.F. Zhang, L.X. Chen, X. Liu, W.Q. Zhang, Effective removal of azo-dye orange II from aqueous solution by zirconium-based chitosan microcomposite adsorbent, RSC Adv., 5 (2015) 93840–93849.
[52] X.Y. Jin, B. Yu, Z.L. Chen, J.M. Arocena, R.W. Thring, Adsorption of Orange II dye in aqueous solution onto surfactant-coated zeolite: Characterization, kinetic and thermodynamic studies, J. Colloid Interf. Sci., 435 (2014) 15–20.